Photodiagnosis and Photodynamic Therapy 28 (2019) 292–296

Contents lists available at ScienceDirect

Photodiagnosis and Photodynamic Therapy

journal homepage: www.elsevier.com/locate/pdpdt

A comparative study of machine learning classifiers for risk prediction of asthma disease

Rahat Ullah[a,*], Saranjam Khan[b], Hina Ali[a], Iqra Ishtiaq Chaudhary[c], Muhammad Bilal[a], Iftikhar Ahmad[d,*]

[a] Agri. & biophotonics Division, National Institute of Lasers & Optronics, Islamabad, Pakistan
[b] Department of Physics, Islamia College Peshawar, Pakistan
[c] Department of Bioinformatics and Biotechnology, International Islamic University, Islamabad, Pakistan
[d] Institute of Radiotherapy and Nuclear Medicine (IRNUM), Peshawar, Pakistan

ARTICLE INFO

Keywords:
Raman spectroscopy
Asthma disease
Machine learning algorithms
Risk prediction

ABSTRACT

Asthma is a chronic disease characterized by wheezing, chest tightening and difficulty in breathing due to inflammation of lung airways. Early risk prediction of asthma is crucial for proper and effective management. This study presents the use of machine learning approach for risk prediction of asthma by evaluating Raman spectral variations between asthmatic as well as healthy sera samples. Specifically, Raman spectra from 150 asthma and 52 healthy control blood sera samples were acquired. Spectral analyses illustrated significant spectral variations ($p < 0.0001$) in the asthmatic samples when compared with healthy sera. The existing spectral differences were further exploited by using artificial neural network (ANN) along with support vector machine (SVM) and random forest (RF) algorithms towards machine-assisted classification of the two groups. Quantitative comparison of the evaluation metrics of the classification algorithms showed superior performance of SVM model. Our results indicate that Raman spectroscopy in tandem with SVM can be used in the diagnosis and machine-assisted classification of asthma patients with promising accuracy.

1. Introduction

Asthma is a chronic disease which arises due to blockage of airways in the lungs. The characteristic symptoms of asthma are wheezing, chest tightness and difficulty in breathing [1]. Pathophysiological changes appeared in asthma are due to the interaction between different cells, cytokines and cellular elements. Such molecular interaction activates a number of inflammatory cytokines e.g. interleukin (IL) 4,9,13 and effector cells due to T-helper type-2 cells (Th2), which triggers the immunological response followed by obstruction of airflow [2–4]. It is one of the most prevalent inflammatory diseases in humans, affecting peoples of all ages and cultural groups [5]. It is ranked 28th among the leading causes of disease burden globally, particularly in low- and middle-income countries (LMICs). According to 2016 report, the asthma disease affected around 340 million people around the world [7]. Mortality and morbidity rates of asthma are increasing day by day globally. The average annual prevalence rate of asthma is higher in kids (9.5%) than adults (7.7%) [8].

Generally, the diagnosis of asthma is built on clinical signs and symptoms. It requires a complete medical assessment and physical inspection alongside of a lung function test. While the lung function test is difficult to execute in children particularly with ages around five years. Most often, the differential opinion of asthma becomes difficult due to the similarity of the symptoms with many other lung diseases. Such confusions can lead to the misdiagnosis of asthma such as bronchiolitis or with pneumonia (common cold). Hence, identification of asthma particularly in infants is still a challenge for clinicians [1,9]. Once established, the treatment of asthma is relatively slow and based on measure of severity of the disease instead of its pathophysiology. The damaged caused by the inflammation or the disorder of the airways is somehow reversible. In some asthmatic patients, the reversibility may be incomplete and cannot be fully cured [10]. Early identification and prevention of such chronic and most prevalent diseases is highly appreciable as well as crucial for disease management authorities [11–13]. False or less accurate prediction might cause overtreatment of higher percentages of people or under treatment of several others [14].

Machine learning is a set of statistical tools or techniques that are very helpful because it analyze the data in different perspective and provide useful information [15]. These techniques are able to discover concealed information from a vast amount of disease-related records. A

* Corresponding authors.
E-mail addresses: rahat_khalil@yahoo.com (R. Ullah), iahmadmp@gmail.com (I. Ahmad).

https://doi.org/10.1016/j.pdpdt.2019.10.011
Received 23 August 2019; Received in revised form 2 October 2019; Accepted 7 October 2019
Available online 12 October 2019
1572-1000/ © 2019 Elsevier B.V. All rights reserved.

number of models are available for predicting disease risk based on immense physical examinations data [11,16]. Such techniques overcome the limitations of human error and subjectivity, and are used in process of decision making based on the knowledge learned by input data [17]. Using machine learning approaches for early asthma risk prediction can prevent and manage the disease burden in a systematic way. People who are at high risk of developing asthma will be identified well before the onset of the disease. Prior identification of the risk leads to the timely prevention of the disease and can significantly reduce the rates of asthma prevalence. Which in turn, reduce the load on clinician particularly in making decision regarding infants, improving the patient's life quality and contribute to the limited and responsible utilization of health resources [18].

In current study, three well-accepted classification algorithms are applied on asthmatic patient's data sets for disease risk prediction. These algorithms includes support vector machine (SVM) along with artificial neural network (ANN) and random forest (RF). The Raman spectral data acquired from asthmatic as well as control blood sera were fed to these classifiers. The outcome of this study is to obtain an optimized classifier among the above by comparing their results for asthma risk prediction. Hence, Raman spectral data together with such an optimized machine algorithm will help in executing real time classification. It is also intended to extend the same approach for further diseases as well.

2. Material and methods

2.1. Blood collection and serum preparation

On the whole blood samples of 150 asthmatic patients were gathered at Pakistan Institute of Medical Sciences (PIMS) hospital, Islamabad. Additionally, blood samples from 52 healthy volunteers were also collected as control. The demographic analysis and clinical characteristics of patients along with complete history were noted on proper questionnaire formatted for research activities. It includes different parameters like name of patient, age of the patient, gender, lifestyle, other allergic diseases and the condition of disease. Patients with missing data are not included in the present study. The participants (including parents and their children) shared useful information by answering questions like asthma and other allergic symptoms, wheezing episodes, family history, parental history, and so on. Table 1 depicts the age as well as gender distribution of the overall patients.

From each individual, blood sample was collected in gel tube (gel& clot activator, ImuMed, Germany). All samples were positioned upright for about 30 min at room temperature and allowed to clot before serum extraction. All samples were then centrifuged using Hettich Centrifuge D-7200, Germany operated at 3500 rpm for 10 min. After centrifugation, the supernatant sera were immediately transferred to 1.5 ml aliquot tubes with the help of pipette, labeled and stored at −16 °C until further use. During the whole exercise i.e. from patients' blood collection to sera extraction, precautionary measures were strictly followed.

2.2. Acquisition of Raman spectra and its data processing

After thawing, from each serum sample a drop of 30 μl was put on glass slide and allowed the water moisture to evaporate under room temperature. In semi-dried condition, Raman spectra was acquired from every single sample using μRamboss (DONGWOO OPRTON, South Korea) Raman spectrometer with 4 cm^{-1} resolution as described in [19]. A continuous laser system of 532 nm wavelength and 40 mW power at sample surface is used as an excitation source. The power of the laser source was so chosen as to avoid any photo-degradation of the sample. Every sample was exposed five times at different location and averaged to include representation from the whole sample. The exposure time was set at 5 s throughout. An objective lens of 100x magnification and numerical aperture of 0.7 is used for focusing and collection of Raman signals; with such microscopic lens, the laser beam was tightly focused (i.e., beam diameter ˜ micrometer). Raman spectral data was acquired on the entire detector range i.e. −32 to 1836 cm^{-1} but only the region from 600–1700 cm^{-1} has been used for subsequent spectral analysis in this study.

The Raman spectra acquired from the sera samples contained considerable noise and inherent fluorescence from the naturally available fluorophores, which significantly compromise the weak Raman signal, necessitating pre-processing of the raw spectra before the analyzing the possible differences in the spectra from the sera samples in the two groups. The average Raman spectra from each sera sample was smoothed, baseline corrected and normalized in the MATLAB environment. Afterwards, a mean representative Raman spectrum of both the asthma and normal groups was obtained by averaging out the normalized Raman spectra of all individual samples in the respective group, as shown in Fig. 2.

2.3. Classification algorithms

After spectra acquisition and data preprocessing, the next step was to develop, evaluate, and compare different computer assisted multivariate models for classification of the healthy and asthma samples by highlighting the differences in their Raman spectra. Albeit several classification algorithms have been suggested and implemented in the framework of biomedical optics, only three such algorithms were selected due to their accurate classification capability as well as their quick response. Specifically, we developed custom models of artificial neural network (ANN), support vector machine (SVM) and random forest (RF) algorithms to automatically classify between healthy and asthma samples. Details of these algorithms can be seen elsewhere [6,20,21]. To facilitate a one-to-one comparison, the 10-fold cross-validation model was used for all three classification algorithms. The quantitative comparison was carried out by the corresponding evaluation metrics of sensitivity (S_n), specificity (S_p), positive predictive value (PPV), negative predictive value (NPV), accuracy (Acc), Mathew's correlation coefficient (MCC), and receiver operator characteristic (ROC) curve for each algorithm. To facilitate understanding of the reader, Fig. 1 shows the overview of the methodology used in this study in the form of a schematic flow chart.

3. Results and discussion

3.1. Data analysis

Blood serum of asthmatic individuals is analyzed for optical diagnosis using Raman spectroscopy. Serum extracted from human blood is a biofluid that contains a variety of different biomolecular constituents including lipids and fats, a variety of vitamins and minerals, glucose and immunoglobulin [19]. All biological samples exhibit different Raman spectra comprised of several Raman peaks. Each peak is assigned to a biomolecule on the basis of their specific vibration sequence [22]. Fig. 2 shows the Raman spectra of healthy and asthmatic blood sera. For demonstration purpose, normalized mean Raman spectra of healthy group are shown in black color, whereas, asthmatic group are shown in red color.

On comparison of the diseased and normal samples, almost similar

Table 1
Age and gender wise sampling distribution of asthmatic patients and healthy volunteers.

	Males	Females	Age (years)	
			Range	Mean
Asthmatic	83	67	27-65	46
Healthy	23	29	23-53	38

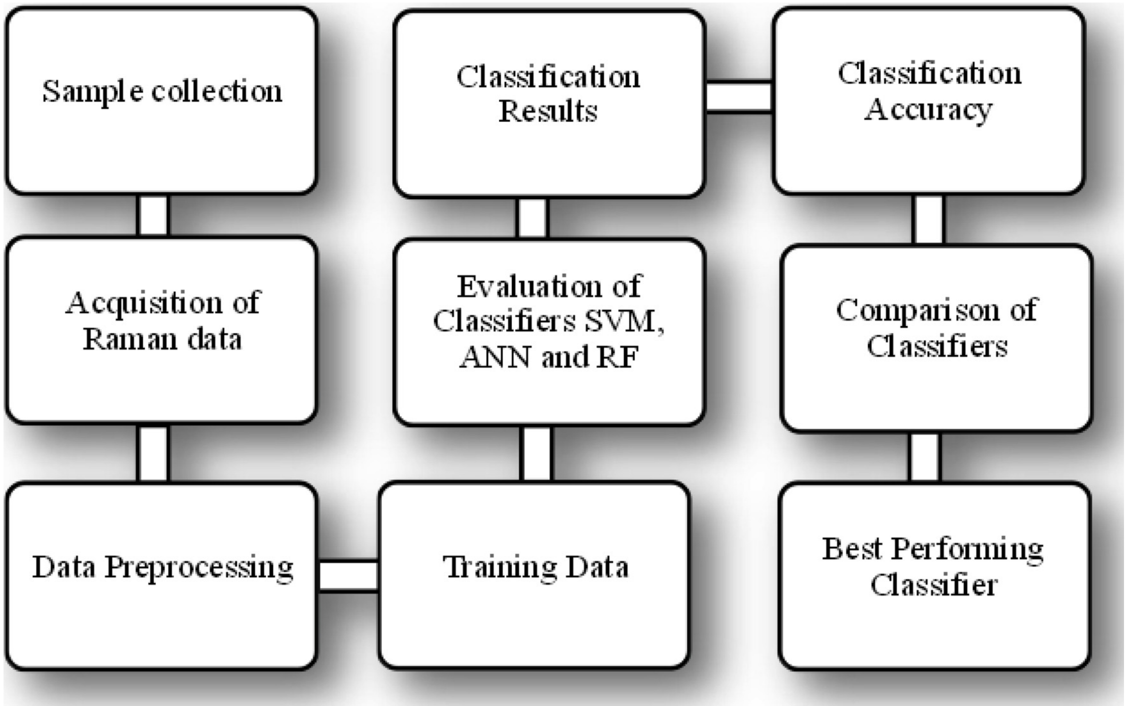

Fig. 1. Schematic flowchart showing the summary of the methodology used in this study.

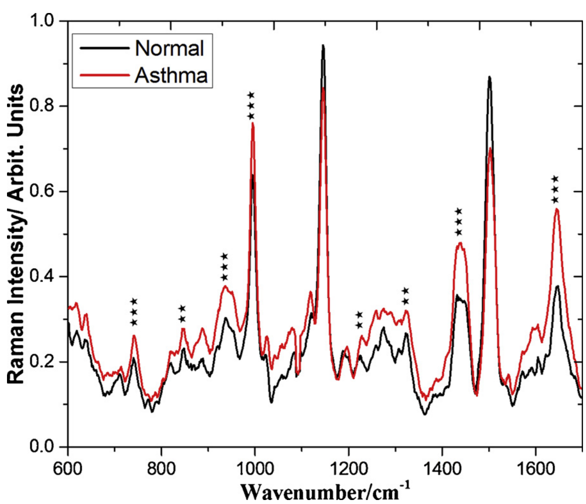

Fig. 2. Mean Raman spectra of blood sera for healthy control (black pseudo color) and asthma patients (red pseudo color). The overall Raman spectral data acquired from all sera samples are off (blue shifted) by 6-7 cm^{-1} due to system calibration. ★★ = p value < 0.01; ★★★ < 0.001, calculated with two-tail unpaired t-test; n (normal) = 52, n (asthma) = 150.

pattern was observed, however there is a major difference in Raman shifts intensity. Raman spectra of healthy sera, shows three very distinct and noticeable Raman peaks arises at 998 cm^{-1} which is assigned to phenylalanine and peaks at shift position 1150 and 1510 cm^{-1} assigned to carotenoids [23]. These Raman peaks are well preserved and reproducible. Excitation at 532 nm results in strong enhancement of these Raman peaks. In diseased sera samples, the peaks at shift position 1150 and 1510 cm^{-1} are somehow diminishing or repressing. In contrast, novel peaks are appeared at diverse locations for example at 749, 824, 844, 923–947, 1198, 1228, 1325, 1437 and 1647 cm^{-1} as clearly seen in Fig. 2. The overall Raman spectral data acquired from all sera samples are off (blue shifted) by 4–7 cm^{-1} due to system calibration. The calibration curve of silicon confirmed this blue shifted offset which can be seen in supporting document (Fig. 1S). The observed variety of additional peaks could be ascribed to the increased immune hyper-response in rigorous asthma attacks that might direct the elevated secretion of certain biomolecule like serum protein albumin and immunoglobulin comparative to carotenoids.

The characteristic peak observed at 998 cm^{-1} arises due to phenylalanine's breathing mode of benzene symmetric ring available in proteins [23]. Comparison of control and diseased sera samples shows an

Table 2
Summary of the peak position, peak values, *p*-values and confidence intervals for the Raman spectra of healthy and asthma samples.

Sr. No.	Peak Position	Peak Value		*p* value (CI)
		Normal	Asthma	
1	750	0.155	0.214	0.0008 (−0.093 −0025)
2	830	0.172	0.220	0.0054 (−0.082 to −0.014)
3	930	0.262	0.362	< 0.0001 (−0.143 to −0.057)
4	998	0.580	0.686	< 0.0001 (−0.157 to −0.054)
5	1156	0.422	0.417	0.775 (−0.029 – 0.39)
6	1190	0.224	0.214	0.488 (-0.018 - 0.038)
7	1230	0.198	0.254	0.003 (−0.093 to −0.019)
8	1330	0.347	0.282	0.005 (0.020 – 0.111)
9	1430	0.215	0.461	< 0.0001 (−0.300 to −0.191)
10	1515	0.429	0.430	0.956 (-0.038 – 0.036)
11	1656	0.277	0.435	< 0.0001 (−0.222 to −0.094)

Table 3
Confusion matrix of various classification algorithms evaluating the differences in mean Raman spectra of blood sera from healthy and asthma samples.

Classifier	Asthma sample	Normal sample	
Artificial Neural Network	142	8	Asthma sample
	8	44	Normal sample
Support Vector Machine	147	3	Asthma sample
	9	43	Normal sample
Random Forest	146	4	Asthma sample
	12	40	Normal sample

Table 4
Evaluation metrics for various classification algorithms used for machine assisted differentiation of sera samples from healthy controls and asthma patients.

Classifier	S_n	S_p	*PPV*	*NPV*	*Acc*	*F measure*	*MCC*	*ROC* Area
Neural Network	0.947	**0.846**	**0.947**	0.846	0.921	0.947	0.793	**0.965**
Support Vector Machine	**0.980**	0.827	0.942	**0.935**	**0.941**	**0.961**	**0.841**	0.903
Random Forest	0.973	0.769	0.924	0.909	0.921	0.948	0.787	0.952

S_n = Sensitivity; S_p = Specificity; *PPV* = Positive Predictive Value; *NPV* = Negative Predictive Value; *Acc* = Accuracy; *MCC* = Mathew's Correlation Coefficient; *ROC* = Receiver Operator Characteristic.

increase in intensity at this peak position. Our result depicts a noticeably increased level of this important agent in asthmatic sera samples as compared to the healthy samples. Studies have shown that phenylalanine is among the nine most essential amino acids which are involved in protein synthesis as well as tyrosine formation inside the liver. The metabolism of phenylalanine depends strongly on integrity of liver cells. Any defect or degradation of enzymes in hepatocytes i.e. liver cell injury could elevate its concentration in the sera [24,25]. It is well established that in asthmatic patient's liver as well as kidney start mal functioning, hence could be one of the reason for an elevated phenylalanine level in the sera.

Furthermore, the presence of the other prominent Raman peaks at 1150 and 1510 cm^{-1} are assigned to β-carotene [23,26]. The most important job of this agent is to prevent damage in cell DNA in context of lipid per oxidation. Other studies also presented the role of β-carotene in the prevention of many physiological disorders, for example cardiac diseases, infection in respiratory system, diarrhea, diseases in immune system, asthma etc. [22]. A strong association is revealed between reduced levels of β-carotene (serum vitamin-A) and severe airway blockage in adults [23,27]. Recent study has shown a decrease in the serum vitamin-A/β-carotene levels in children having asthma [28]. Our results also clearly show a decrease in β-carotene in diseased samples when compared to the normal. The analysis of these molecular fingerprints shows a clearly reduced ratio of carotenoid between healthy and diseased blood sera. While, the Raman peaks appear at spectral position 740 (assigned to Tryptophan), bands at 824 and 844 (assigned to Tyrosine), 923 and 947 (C—C bond of peptide backbone), 996 (Phenylalanine), 1437 (assigned to lipids) and 1647 cm^{-1} (amide I of peptide backbone) are all belongs to protein structure [29]. Such findings possibly will assist clinicians in non-invasive identification and differentiation diagnosis of asthma based on Raman technique.

3.2. Development of the classification models

For machine assisted classification of the asthma and healthy control samples, we developed the custom models of artificial neural network (ANN), support vector machine (SVM) and random forest (RF) classifiers in MATLAB environment. In the first step, the mean Raman spectrum from both the asthma and healthy control samples was carefully analyzed to identify the differences that can be used as fingerprints of the samples and exploited for their classification. We identified 11 peaks at different shift positions in the Raman spectra of infectious and healthy groups with prominent differences and assessed the statistical significance of these spectral differences with unpaired student t-test. It was found that the spectral differences in 05 (out of 11) peaks were extremely significant with $p < 0.0001$, highly significant for 03 (out of 11) peaks while the difference in the remaining 03 peaks was not statistically significant. The peak positions in the two spectra, their differences, and the calculated p values along with the corresponding 95% confidence interval (CI) have been summarized in Table 2. In the second step, all the three algorithms (i.e., ANN, SVM and RF) were used to classify the sera samples of the two groups on the basis of the 08 Raman spectral peaks; each algorithm was trained on the 08 peaks with 10-fold cross-validation scheme, followed by the prediction/ classification of the samples.

3.3. Evaluation and comparison of the classification models

The performance of all three developed models i.e., ANN, SVM and RF for classification of the samples in the two groups was assessed through the generated confusion matrix, as depicted in Table 3. The correctly classified healthy control vs. asthma samples by the ANN, SVM and RF classifier were 44/52 vs. 142/150, 43/52 vs. 147/150 and 40/52 vs. 146/152, respectively. To quantitatively evaluate and compare the performance of these classifiers, different metrics were calculated from the confusion matrix (Table 3), which include the sensitivity (S_n), specificity (S_p), positive predictive value (*PPV*), negative predictive value (*NPV*), accuracy (*Acc*), Mathew's correlation coefficient (*MCC*), and receiver operator characteristic (*ROC*) curve, as presented in Table 4. From the comparison of the evaluation metrics of the three classifiers, it is clear that the SVM-based classification of the samples in the two groups is better than ANN and RF. Specifically, the SVM performed better in terms of S_n (= 98.0%), *NPV* (= 93.5%), *Acc* (= 94.1%), *F measure* (= 96.1%) and *MCC* (= 84.1%), while the ANN provides superior S_p (= 84.6%), *PPV* (= 94.7%) and area under *ROC* curve (= 96.5%. It may be noted that the two metrics (i.e. S_p and *PV*) for ANN are only marginally better than the corresponding metrics for SVM. The classification performance of RF algorithm was relatively poor, as revealed from the comparison of the evaluation metrics in Table 4.

4. Conclusion

Integration of machine learning algorithm with medical care systems would facilitate in improving the efficacy and competence of healthcare industry. The average cost of medical organizations can be effectively reduced by utilizing such computer aided support systems for making decisions. Comparative analysis of the results of different classification algorithms (i.e., ANN, SVM and RF) showed that SVM is a more suitable technique for the classification of asthma, as the comparison showed its superior evaluation metrics for sensitivity, accuracy, negative predictive value and Mathew's correlation coefficient. Chronic and highly prevalent infectious diseases like asthma could be managed at early stage by implementing such data classification techniques for screening purposes.

Appendix A. Supplementary data

Supplementary material related to this article can be found, in the online version, at doi:https://doi.org/10.1016/j.pdpdt.2019.10.011.

References

[1] E. Chatzimichail, E. Paraskakis, M. Sitzimi, A. Rigas, An intelligent system approach for asthma prediction in symptomatic preschool children, Comput. Math. Methods Med. (2013).
[2] A. Shifren, C. Witt, C. Christie, M. Castro, Mechanisms of remodeling in asthmatic airways, J. Allergy (Cairo) (2012) 316049.
[3] J. Lötvall, C.A. Akdis, L.B. Bacharier, L. Bjermer, T.B. Casale, A. Custovic, R.F. Lemanske Jr, A.J. Wardlaw, S.E. Wenzel, P.A. Greenberger, Asthma endotypes: a new approach to classification of disease entities within the asthma syndrome, J. Allergy Clin. Immunol. 127 (2) (2011) 355–360.
[4] W.C. Moore, D.A. Meyers, S.E. Wenzel, W.G. Teague, H. Li, X. Li, B. Gaston, Identification of asthma phenotypes using cluster analysis in the severe asthma

research program, Am. J. Respir. Crit. Care Med. 181 (4) (2010) 315–323.
[5] P.J. Barnes, K.F. Chung, C.P. Page, Inflammatory mediators of asthma: an update, Pharmacol. Rev. 50 (4) (1998) 515–596.
[6] R. Ullah, S. Khan, F. Farman, M. Bilal, C. Krafft, S. Shahzad, Demonstrating the application of Raman spectroscopy together with chemometric technique for screening of asthma disease, Biomed. Opt. Express 10 (2) (2019) 600–609.
[7] T. Vos, A.A. Abajobir, K.H. Abate, Global, regional, and national incidence, prevalence, and years lived with disability for 328 diseases and injuries for 195 countries, 1990–2016: a systematic analysis for the Global Burden of Disease Study 2016, Lancet 390 (10100) (2017) 1211–1259.
[8] P.A. Loftus, S.K. Wise, Epidemiology of asthma, Curr. Opin. Otolaryngol. Head Neck Surg. 24 (3) (2016) 245–249.
[9] J.A. Castro-Rodriguez, L. Garcia-Marcos, J.D.A. Rojas, J. Valverde-Molina, M. Sanchez-Solis, Mediterranean diet as a protective factor for wheezing in preschool children, J. Pediatr. 152 (6) (2008) 823–828.
[10] J.V. Fahy, Type 2 inflammations in asthma—present in most, absent in many, Nat. Rev. Immunol. 15 (1) (2015) 57.
[11] R. Li, W. Liu, Y. Lin, H. Zhao, C. Zhang, An ensemble multilabel classification for disease risk prediction, J. Healthc. Eng. (2017).
[12] J.A. Castro-Rodriguez, S.L. Cifuentes, C.E. Rodr´ıguezMart´ınez, The asthma predictive index remains a useful tool to predict asthma in young children with recurrent wheeze in clinical practice, J. Allergy Clin. Immunol. 127 (4) (2011) 1082–1083.
[13] D.G. Panazzolo, F.L. Sicuro, R. Clapauch, P.A. Maranhao, E. Bouskela, L.G. Kraemer-Aguiar, Obesity, metabolic syndrome, impaired fasting glucose, and microvascular dysfunction: a principal component analysis approach, BMC Cardiovasc. Disord. 12 (2012) 102.
[14] A. Helmy, C.A. Antoniades, M.R. Guilfoyle, K.L. Carpenter, P.J. Hutchinson, Principal component analysis of the cytokine and chemokine response to human traumatic brain injury, PLoS One 7 (2012) 39677.
[15] S. Sakr, R. Elshawi, A.M. Ahmed, W.T. Qureshi, C.A. Brawner, S.J. Keteyian, M.H. Al-Mallah, Comparison of machine learning techniques to predict all-cause mortality using fitness data: the Henry ford exercIse testing (FIT) project, BMC Med. Inform. Decis. Mak. 17 (1) (2017) 174.
[16] J. Finkelstein, Machine learning approaches to personalize early prediction of asthma exacerbations, Ann. N. Y. Acad. Sci. 1387 (1) (2017) 153–165.
[17] I.R. Vashi, S. Mishra, S. Andhariya, A comparative study of classification algorithms for diseases prediction in medical domain, Asian J. Convergence Technol. (2017) 3.
[18] D. Sanchez-Morillo, M.A. Fernandez-Granero, A. Leon-Jimenez, Use of predictive algorithms in-home monitoring of chronic obstructive pulmonary disease and asthma: a systematic review, Chron. Respir. Dis. 13 (3) (2016) 264–283.
[19] M. Bilal, R. Ullah, S. Khan, H. Ali, M. Saleem, M. Ahmed, Lactate based optical screening of dengue virus infection in human sera using Raman spectroscopy, Biomed. Opt. Express 8 (2) (2017) 1250–1256.
[20] I. Ullah, I. Ahmad, H. Nisar, S. Khan, R. Ullah, R. Rashid, Hassan Mahmood computer assisted optical screening of human ovarian cancer using Raman spectroscopy, J. Photodiagn. Photodyn. Ther. 15 (2016) 94–99.
[21] S. Khan, R. Ullah, S. Shahzad, N. Anbreen, M. Bilal, A. Khan, Analysis of tuberculosis disease through Raman spectroscopy and machine learning, J. Photodiagn. Photodyn. Ther. 24 (2018) 286–291.
[22] P. Arora, V. Kumar, S. Batra, Vitamin A status in children with asthma, Pediatr. Allergy Immunol. 13 (3) (2002) 223–226.
[23] J. De Gelder, K. De Gussem, P. Vandenabeele, L. Moens, Reference database of Raman spectra of biological molecules, J. Raman Spectrosc. 38 (9) (2007) 1133–1147.
[24] S. Neumann, H. Welling, S. Thuere, Evaluation of serum L-phenylalanine concentration as Indicator of liver disease in dogs: a pilot study, J. Am. Anim. Hosp. Assoc. 43 (2007) 193–200.
[25] J.H. James, V. Ziparo, B. Jeppson, J.E. Fisher, Hyperammonaemia, plasma aminoacid imbalance, and blood-brain aminoacid transport: a unified theory of portalsystemic encephalopathy, Lancet 314 (8146) (1979) 772–775.
[26] R. Ullah, S. Khan, S. Javaid, H. Ali, M. Bilal, M. Saleem, M. Ahmed, Raman spectroscopy combined with a support vector machine for differentiating between feeding male and female infants mother's milk, Biomed. Opt. Express 9 (2) (2018) 844–851.
[27] A. Morabia, M.J. Menkes, G.W. Comstock, M.S. Tockman, Serum retinol and airway obstruction, Am. J. Epidemiol. 132 (1) (1990) 77–82.
[28] A.M. Al-Senaidy, Serum vitamin a and β-Carotene levels in children with asthma, J. Asthma 46 (2009) 699–702.
[29] C. Krafft, K. Wilhelm, A. Eremin, S. Nestel, N. von Bubnoff, W. Schultze-Seemann, J. Popp, I. Nazarenko, A specific spectral signature of serum and plasma-derived extracellular vesicles for cancer screening, Nanomed. Lond. 13 (3) (2017) 835–841.